The influence of an electric field on the electronic structure of a surface containing defects: an embedding-potential approach

1997 J. Phys.: Condens. Matter 9 1793

(http://iopscience.iop.org/0953-8984/9/8/010)

J. Phys.: Condens. Matter **9** (1997) 1793–1811. Printed in the UK PII: S0953-8984(97)78172-4

The influence of an electric field on the electronic structure of a surface containing defects: an embedding-potential approach

H Ness and A J Fisher

Department of Physics and Astronomy, University College London, Gower Street, London WC1E 6BT, UK

Received 26 September 1996, in final form 13 December 1996

Abstract. We study the effect of an idealized tip-induced electric field on the electronic structure of a semiconductor surface containing defects. The embedding-potential method is used to connect the Green's functions of the solid and the vacuum. The corresponding localized perturbation potential permits us to derive the Dyson equation for the Green's function of the full system. This equation is solved in real space on a discrete mesh. The polarization of the surface with defects is determined inside the tunnelling barrier. It is found that the electronic density over the clean surface responds more strongly to the tip-induced electric field than the electronic density over the region containing defects.

1. Introduction

Scanning tunnelling microscopy (STM) [1] is now a well established tool for obtaining images of surfaces at the atomic scale. Different models have been developed to explain the STM contrast. These arise from perturbation theory [2] or treat the scattering phenomenon inside the tunnelling junction more accurately [3]. It is apparent that most of these models are based on zero- (electric-) field calculations. However, it is increasingly recognized that, under particular conditions, tip–sample interactions such as the tip inducing an electric field can play an important role.

In a recent paper, we investigated the contrast in STM images of a Si(001) surface on which ethylene (C_2H_4) molecules were adsorbed [4]. The experiments [5, 6] produced STM images for constant tunnel current in which the adsorbed molecules appeared slightly darker than the bare silicon dimers when tunnelling out of the surface. We found that it was necessary to account in our *ab initio* calculations not only for (i) the geometrical structure of the system and (ii) the electronic structure of the unperturbed surface, but also (iii) the modification of this electronic structure by the tip-induced electric field. Specifically, this electric field had the effect of withdrawing electrons from the surface more strongly over the bare silicon dimers than over the adsorbed molecules; this reversed the contrast of the zero-field image in which the molecules were (incorrectly) predicted to be brighter than the bare dimers.

This result can be interpreted as follows. The silicon substrate is more polarizable than the alkene molecules which are deposited on it; it therefore seems reasonable that electrons tunnelling into the vacuum above the bare surface respond more strongly to screen out the applied field. However, applying the concept of polarizability to the tunnelling electrons

0953-8984/97/081793+19$19.50

involves extending it beyond its normal domain of validity. In the present paper, therefore, we discuss a simple model of the situation in which we neglect all effects arising from the atomic geometry, and concentrate entirely on the electronic structure and the effect of the electric field upon it. Specifically, we represent the molecule as a region of locally increased band gap (and hence, to use our previous language, reduced polarizability) on the semiconductor surface. We neglect also the effects of the electric field within the material and concentrate entirely on its influence on the wave functions in the vacuum. We show that, in the energy range relevant for the experiments, the electron density (and tunnelling current density) near the molecule is suppressed relative to that at the bare surface; this is to be expected (although in the experiments and the full calculations this effect is somewhat compensated by the fact that the molecules stand above the level of the rest of the surface). However, our results also show that the relative suppression of electron tunnelling over the molecule *increases* as the field is raised. This confirms the validity of the simple picture presented earlier: the electrons over the clean surface are responding more strongly to the applied field.

We perform our calculations using a Green's function technique associated with the embedding method of Inglesfield [7] in order to determine the electronic density of our model adsorbate–surface system. This work is also based on an equivalent version of the scattering approach developed by Lucas *et al* [8] which has been used to study elastic tunnelling in STM.

The paper is organized as follows. In section 2, we give a brief summary of the general approach to the embedding-potential method. The model used to describe the adsorbate–surface system is presented in section 3, together with the basic Dyson equation needed to determine the electronic density of such a system. We derive the expression for the Green's function of the bare surface in the presence of an external electric field in section 4. The forms of the embedding potentials are given in section 5. The Dyson equation is solved using a discretization scheme (section 6). We also derive the solution of such an equation in the case of a particular symmetry of the adsorbate (section 7). The electronic density of the system and more especially its modifications due to the presence of the electric field are presented in section 8. Finally we summarize the most significant results that we have obtained, and discuss improvements and other applications of the method (section 9).

2. The embedding potential and the effective Hamiltonian: the general case

We consider a system (filling the whole space) which can be divided into two parts: a limited region of space (region I) and the rest of the space (region II). Representative cases for this situation are for example an impurity in an infinite crystal, and the surface of a semi-infinite crystal. The basic idea of the embedding method is to solve the problem in the *perturbed* region of the crystal (region I) by adding to the corresponding Hamiltonian an effective potential defined on the surface S separating regions I and II. The presence of this surface potential (the embedding potential) automatically ensures that the wave functions of region I match onto the rest of the space (region II). The embedding method is reminiscent of standard Green's-function-matching techniques [9–11]. For example, the embedding potential that we present below is equivalent to the real-space representation of the X-operators introduced by Noguera in her theoretical approach to STM [12].

Starting from the original paper by Inglesfield [7], we can derive the effective Hamil-

tonian equation for the Green's function $G(\boldsymbol{r}, \boldsymbol{r}', E)$ of region I as follows:

$$\left(-\frac{1}{2}\nabla_r^2 + V(\boldsymbol{r}) - E\right)G(\boldsymbol{r}, \boldsymbol{r}', E) + \frac{1}{2}\delta(\boldsymbol{n} - \boldsymbol{n}_S) \times \left[\frac{\partial}{\partial \boldsymbol{n}_S}G(\boldsymbol{r}, \boldsymbol{r}', E) + 2\int_S \mathrm{d}^2\boldsymbol{r}_S''\ \Sigma(\boldsymbol{r}_S, \boldsymbol{r}_S'')G(\boldsymbol{r}_S'', \boldsymbol{r}', E)\right] = -\delta(\boldsymbol{r} - \boldsymbol{r}'). \tag{1}$$

The vectors $\boldsymbol{r}$ and $\boldsymbol{r}'$ are located inside region I. $\boldsymbol{r}_S$ and $\boldsymbol{r}_S''$ are vectors lying on the surface S, and $\boldsymbol{n}_S$ is the normal vector of this surface.

The general expression for the embedding potential Σ defined on the separation surface S is

$$\Sigma(\boldsymbol{r}_S, \boldsymbol{r}_S'') = \int_S \mathrm{d}^2\boldsymbol{r}_S'\ G_0^{-1}(\boldsymbol{r}_S, \boldsymbol{r}_S')\left[\delta(\boldsymbol{r}_S' - \boldsymbol{r}_S'') - \frac{1}{2}\frac{\partial}{\partial \boldsymbol{n}_S''}G_0(\boldsymbol{r}_S', \boldsymbol{r}_S'')\right] \tag{2}$$

where $G_0(\boldsymbol{r}, \boldsymbol{r}')$ is in principle any Green's function of the entire system (regions I and II) in the sense that the potential in region II should not be modified by the choice made as regards filling region I. It is often convenient to use for G_0 the Green's function corresponding to region II filling all of the space (this would correspond to an infinite perfect crystal in the example above).

If G_0 is chosen to satisfy the von Neumann boundary condition

$$\frac{\partial}{\partial \boldsymbol{n}_S'}G_0(\boldsymbol{r}_S, \boldsymbol{r}_S') = 0 \tag{3}$$

on the surface S, then the embedding potential takes the simple form

$$\Sigma(\boldsymbol{r}_S, \boldsymbol{r}_S') = G_0^{-1}(\boldsymbol{r}_S, \boldsymbol{r}_S'). \tag{4}$$

However, if we choose instead the Dirichlet boundary condition $G_0(\boldsymbol{r}_S, \boldsymbol{r}_S') = 0$, then by reworking the formalism from the beginning as in [7], it can be shown [14] that the embedding potential can be expressed as

$$\Sigma(\boldsymbol{r}_S, \boldsymbol{r}_S') = -\frac{1}{4}\frac{\partial^2}{\partial \boldsymbol{n}_S\, \partial \boldsymbol{n}_S'}G_0(\boldsymbol{r}_S, \boldsymbol{r}_S'). \tag{5}$$

Formally, since we consider the same physical system, the expressions (4) and (5) for the embedding potential are equivalent. These potentials are calculated in a different way from the different Green's functions (obeying different boundary conditions) but for the same system. The question of the validity of this equivalence of the embedding potentials for different boundary conditions has been addressed by different authors [12, 13]. The equivalence of the embedding potentials defined by equations (2), (4) and (5) is reminiscent of the elegant demonstration given by Tekman of the calculation of the probability of transmission between two half-spaces [13]. It has been shown that the same results are obtained irrespective of the boundary conditions satisfied by the Green's functions on the separation surface. The only relevant boundary conditions are the ones which are satisfied at infinity, that is, outgoing- or ingoing-wave boundary conditions. In the following, we always consider waves (associated with the different regions I and II) propagating in the same direction.

3. The model for the adsorbate–surface system

The general formalism presented in the previous paragraph is well suited to the kind of system that we want to study. The Si(001) surface on which an ethylene molecule is deposited is represented by the following idealized model. The silicon surface is represented by a semi-infinite two-band (valence and conduction) semiconductor (called semiconductor I). The adsorbed molecule is represented by a region of the semiconductor having a larger band gap than the semi-infinite surface. The presence of the adsorbate is localized in a planar region (of arbitrary shape) lying on the surface of semiconductor I. This region will be called the 'defect region' in the following. Then the natural choice for determining the surface S is to take the plane $z = z_0$ to represent the surface of semiconductor I. The two regions delimited by this plane are called for simplicity the left-hand region (semiconductor I) and the right-hand region (the vacuum).

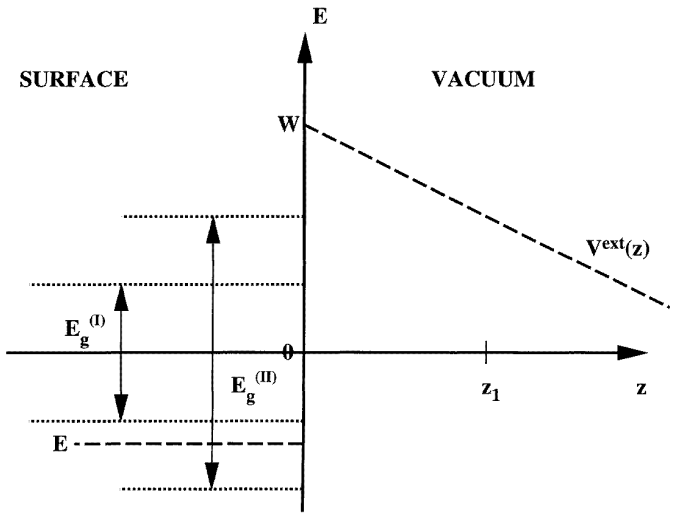

Figure 1. A schematic-diagram energy representation of the surface with defects and the electric field applied in the vacuum.

In the vacuum, we add a linearly decreasing external potential V^{ext} corresponding to the presence of an external electric field. This field represents an idealized tip-induced electric field. As a first approximation we choose a uniform electric field parallel to the surface normal:

$$V^{\text{ext}} = W + \xi^{\text{ext}}(z - z_0). \tag{6}$$

Here W represents the work function of the surface of semiconductor I and ξ^{ext} is the applied electric field. We choose a negative value for ξ^{ext}, which corresponds to an idealized STM experiment in which the electrons tunnel out of the surface. A schematic representation of the present defect–surface system is shown in figure 1.

Now we can apply the formalism developed in section 2 to the present case. It is useful to derive a set of two equations equivalent to equation (1). First we consider the system without the defect region, i.e. only the left-hand region (semiconductor I) and the right-hand region (the vacuum in the presence of the electric field). The equation equivalent

to equation (1) is written as

$$\left(-\frac{1}{2}\nabla_r^2 + V(\boldsymbol{r}) - E\right)G^0(\boldsymbol{r},\boldsymbol{r}',E) + \frac{1}{2}\delta(z-z_0) \times \left[\frac{\partial}{\partial z}G^0(\boldsymbol{r},\boldsymbol{r}',E) + 2\int_S \mathrm{d}^2\boldsymbol{x}''\ \Sigma^0(\boldsymbol{x},\boldsymbol{x}'')G^0(\boldsymbol{x}'',\boldsymbol{r}',E)\right] = -\delta(\boldsymbol{r}-\boldsymbol{r}') \qquad \text{with } \boldsymbol{r},\boldsymbol{r}' \text{ in the right-hand region.} \tag{7}$$

Here $\boldsymbol{x}, \boldsymbol{x}''$ are two-dimensional vectors lying in the surface plane $z = z_0$, G^0 is the Green's function in the vacuum (in the presence of the electric field), and Σ^0 is the embedding potential that permits us to match the wave functions in the vacuum with the electric field (right-hand region) to the wave functions of the two-band semiconductor I (left-hand region). According to the symmetry of the system, equation (6) can be transformed to a one-dimensional problem as shown in the next section.

Next we consider the total system including the defect region on the surface of semiconductor I. An equation similar to equation (7) can be written for the surface with defects:

$$\left(-\frac{1}{2}\nabla_r^2 + V(\boldsymbol{r}) - E\right)G(\boldsymbol{r},\boldsymbol{r}''',E) + \frac{1}{2}\delta(z-z_0) \times \left[\frac{\partial}{\partial z}G(\boldsymbol{r},\boldsymbol{r}''',E) + 2\int_S \mathrm{d}^2\boldsymbol{x}''\ \Sigma(\boldsymbol{x},\boldsymbol{x}'')G(\boldsymbol{x}'',\boldsymbol{r}''',E)\right] = -\delta(\boldsymbol{r}-\boldsymbol{r}''') \qquad \text{with } \boldsymbol{r},\boldsymbol{r}''' \text{ in the right-hand region.} \tag{8}$$

Now multiply equation (7) by $G(\boldsymbol{r}''',\boldsymbol{r})$ and equation (8) by $G^0(\boldsymbol{r}',\boldsymbol{r})$, subtract, and integrate $\boldsymbol{r}$ over the right-hand region, using the fact that the embedding potentials Σ^0 and Σ are symmetric and so, therefore, are the Green's functions G^0 and G, i.e. $G(\boldsymbol{r},\boldsymbol{r}') = G(\boldsymbol{r}',\boldsymbol{r})$ and $\Sigma(\boldsymbol{x},\boldsymbol{x}') = \Sigma(\boldsymbol{x}',\boldsymbol{x})$, to obtain a Dyson equation:

$$G(\boldsymbol{r}',\boldsymbol{r}''',E) = G^0(\boldsymbol{r}',\boldsymbol{r}''',E) + \int_S \mathrm{d}^2\boldsymbol{x}\int_S \mathrm{d}^2\boldsymbol{x}''\ G^0(\boldsymbol{r}',\boldsymbol{x},E)\,\Delta\Sigma(\boldsymbol{x},\boldsymbol{x}'')\,G(\boldsymbol{x}'',\boldsymbol{r}''',E) \tag{9}$$

with $\boldsymbol{r}', \boldsymbol{r}'''$ located in the right-hand region. Here $\Delta\Sigma$ represents the perturbation potential due to the presence of the defect region on the surface plane S. This potential is obtained from the difference of the embedding potentials: $\Delta\Sigma(\boldsymbol{x},\boldsymbol{x}') = \Sigma(\boldsymbol{x},\boldsymbol{x}') - \Sigma^0(\boldsymbol{x},\boldsymbol{x}')$.

The Dyson equation (equation (9)) is the basic formula that we use to determine the electronic density of the defect–surface system and the modifications of such a density according to the value of the external electric field. Before solving this equation, we derive the expressions for the Green's function G^0 and for the embedding potentials.

4. The Green's function G^0 in an external field

Due to the translational invariance in the $\boldsymbol{x}$-direction of the planar surface S, equation (7) can be Fourier transformed according to

$$G^0(\boldsymbol{r},\boldsymbol{r}',E) = G^0(\boldsymbol{x}-\boldsymbol{x}',z,z',E) = \frac{1}{(2\pi)^2}\int \mathrm{d}^2\boldsymbol{k}_\parallel\ g^0(z,z',k_\parallel)\mathrm{e}^{\mathrm{i}\boldsymbol{k}_\parallel\cdot(\boldsymbol{x}-\boldsymbol{x}')} \tag{10}$$

to give for each Fourier component $g^0(z,z')$ the following Green's function equation:

$$\left(\frac{1}{2}k_\parallel^2 - \frac{1}{2}\frac{\mathrm{d}^2}{\mathrm{d}z^2} + V^{\mathrm{ext}}(z) - E\right)g^0(z,z') + \frac{1}{2}\delta(z-z_0)\left[\frac{\mathrm{d}}{\mathrm{d}z}g^0(z_0,z') + 2\Sigma^0(k_\parallel)g^0(z_0,z')\right] = -\delta(z-z') \qquad \text{for } z,z' \geqslant z_0. \tag{11}$$

Note that for simplicity we sometimes drop the energy or $k_\parallel$ (wave-vector) label in the expression for the Green's functions.

The corresponding one-dimensional Schrödinger equation can be reformulated to give the second-order differential equation

$$f''(\zeta) - \zeta f(\zeta) = 0 \tag{12}$$

after the change of variable given by $\zeta = \rho z + \eta$ where

$$\rho = -(2|\xi^{\text{ext}}|)^{1/3} \tag{13}$$

$$\eta = (2|\xi^{\text{ext}}|)^{-2/3}(2(W - E) + k_\parallel^2). \tag{14}$$

Note that we have chosen a negative value for the electric field, and that the planar surface S is located at the origin $z_0 = 0$.

Two independent solutions of equation (12) are known as the Airy functions [15] $\text{Ai}(\zeta)$ and $\text{Bi}(\zeta)$. We wish to consider wave functions propagating out of the surface to the right, since this corresponds to the direction of electron transport when the field is biased in this direction. These wave functions (φ) are obtained as complex linear combinations of the Airy functions, for instance $\varphi(z) = \alpha(\text{Ai}(\zeta) - \text{i}\,\text{Bi}(\zeta))$, α being the normalization constant. In order to show that the φ represent particles travelling to the right, we can calculate the current associated with such wave functions. The one-dimensional current density $j(z)$ associated with a wave function $\Psi(z)$ is expressed as

$$j = \frac{1}{2\text{i}}(\Psi^* \nabla_z \Psi - \Psi \nabla_z \Psi^*). \tag{15}$$

Then choosing $\Psi = \varphi$ and knowing that the Wronskian of the two Airy functions is $W(\text{Ai}(z), \text{Bi}(z)) = \pi^{-1}$, we can find that the current density associated with a wave function φ is given by

$$j = -\pi\alpha^2\rho. \tag{16}$$

Since we consider negative values of the electric field, ρ is by definition (equation (13)) negative and therefore j is positive, meaning that the φ-state propagates to the right. Another important point can be derived from equation (16): it is easily shown that the current density j is simply proportional to the local density of states ($n(E, z) = \int \text{d}\epsilon\ |\varphi(E, z)|^2\delta(\epsilon - E)$) taken in a plane ($z =$ constant) parallel to the surface S. This is why we consider only the effects of the electric field on the local density of states in the following; the z-component of the current density can always be obtained by a simple rescaling.

Then the Green's function $g^0(z, z')$ is constructed from the Airy functions using the standard method to determine a one-dimensional Green's function from an non-homogeneous Sturm–Liouville equation, as can be found for example in [16]. The matching of the wave functions φ to the surface plane $z = z_0$ is obtained via the embedding potential $\Sigma^0(k_\parallel)$. After some algebra, we find that the symmetric Green's function $g^0(z, z')$ is given in the right-hand region by

$$g^0(z, z') = \frac{u(\zeta_>)v(\zeta_<)}{-\frac{1}{2}W(u, v)} \tag{17}$$

where

$$u(\zeta) = \text{Ai}(\zeta) - \text{i}\,\text{Bi}(\zeta) \tag{18}$$

$$v(\zeta) = \text{Ai}(\zeta) + R(\zeta_0)\,\text{Bi}(\zeta) \tag{19}$$

where the Wronskian of the wave functions u and v is

$$W(u, v) = \frac{\rho}{\pi}(R(\zeta_0) + \text{i}). \tag{20}$$

In equation (17), $\zeta_<$ and $\zeta_>$ are respectively the smaller and larger ζ-values associated with z, z' and $\zeta_0 = \rho z_0 + \eta$. In the above equations, R is the complex reflection coefficient

$$R(\zeta_0) = -\frac{\rho\,\mathrm{Ai}'(\zeta_0) + 2\Sigma^0(k_\parallel)\,\mathrm{Ai}(\zeta_0)}{\rho\,\mathrm{Bi}'(\zeta_0) + 2\Sigma^0(k_\parallel)\,\mathrm{Bi}(\zeta_0)} \tag{21}$$

where Ai′ and Bi′ are the derivatives of the Airy functions. The presence of the factor $R(\zeta_0)$ is in principle equivalent to matching the logarithmic derivative of the wave functions φ to the logarithmic derivative of the wave functions of the left-hand region on the surface plane $z = z_0$.

$G^0(\boldsymbol{r}, \boldsymbol{r}')$ is then calculated by Fourier transforming equation (17) as in equation (10). This latter equation can be rewritten as

$$G^0(\boldsymbol{r}, \boldsymbol{r}') = \frac{1}{2\pi}\int_0^\infty \mathrm{d}k_\parallel\; k_\parallel g^0(z, z', k_\parallel) J_0(k_\parallel|\boldsymbol{x} - \boldsymbol{x}'|) \tag{22}$$

since g^0 depends only on the amplitude of the wave vector $\boldsymbol{k}_\parallel$, J_0 being the cylindrical Bessel function of order 0. However, as already noticed by Lucas *et al* [8], the integral in equation (22) presents some numerical convergence difficulties for large $k_\parallel$-values and more especially when $z = z'$. This is due to the slow oscillatory decay behaviour of the Bessel function $J_0(x)$ for large x-values. An acceleration scheme can be introduced. It is based on the fact that for large $k_\parallel$-values, the Green's function g^0 tends towards a corresponding free-electron Green's function g^f. Indeed for very large $k_\parallel$-values, the Green's function equation (11) has the solution $-\exp(-k_\parallel|z - z'|)/k_\parallel$. This idea was introduced by Lucas *et al* [8] for the case in which the unperturbed system contains no electric field. We have checked that it can still be used even with the electric field present; we find that the Green's function tends asymptotically to

$$g^f(z, z') = -\frac{1}{\kappa}\mathrm{e}^{-\kappa|z-z'|} \tag{23}$$

where $\kappa^2 = k_\parallel^2 - 2(E - V^{\mathrm{ext}}(z_<))$ and $z_<$ is the smaller of z, z'. Hence by adding and subtracting the free-electron Green's function g^f in the expression for g^0, we can rewrite equation (22) as

$$G^0(\boldsymbol{r}, \boldsymbol{r}', E) = G^f(\boldsymbol{r}, \boldsymbol{r}', E) + \frac{1}{2\pi}\int_0^{k_\parallel^{\max}} \mathrm{d}k_\parallel\; k_\parallel J_0(k_\parallel|\boldsymbol{x} - \boldsymbol{x}'|)[g^0(z, z', k_\parallel) - g^f(z, z', k_\parallel)] \tag{24}$$

where $k_\parallel^{\max}$ is the value above which the difference term inside the brackets in the integral is negligible. G^f is the two-dimensional Fourier transform of g^f:

$$G^f(\boldsymbol{r}, \boldsymbol{r}', E) = -\frac{1}{2\pi}\frac{\mathrm{e}^{\mathrm{i}K|\boldsymbol{r}-\boldsymbol{r}'|}}{|\boldsymbol{r} - \boldsymbol{r}'|} \tag{25}$$

where $K^2 = 2(E - V^{\mathrm{ext}}(z_<))$. Note that we also consider the corresponding complex K-values when the value of the energy E is lower than the value of the potential $V^{\mathrm{ext}}(z_<)$; these are $K = +\mathrm{i}\sqrt{2(V^{\mathrm{ext}}(z_<) - E)}$.

This special scheme, as already used by Lucas *et al* [8], permits us to obtain an efficient numerical convergence of the integral in equation (22). Then $G^0(\boldsymbol{r}, \boldsymbol{r}')$ is calculated via equation (24).

Now in order to achieve the complete determination of the real-space Green's function $G^0(\boldsymbol{r}, \boldsymbol{r}', E)$ and to start solving the Dyson equation, we have to know the expression for the one-dimensional embedding potential $\Sigma^0(k_\parallel)$ and of the real-space embedding potentials Σ^0 and Σ. Such expressions are derived in the next section.

5. Embedding potentials

We adopt a very simple model for the Green's function for semiconductor I. We write such a Green's function as

$$G_{(\mathrm{I})} = G_c + G_v \tag{26}$$

where G_c is the Green's function for a free-electron-like conduction band with the dispersion relation

$$E = E_c + \frac{1}{2}k^2 \tag{27}$$

and G_v is the Green's function for a free-electron-like valence band with the dispersion relation

$$E = E_v - \frac{1}{2}k^2. \tag{28}$$

It would be straightforward to include different effective masses for the conduction and valence bands, but we have not done this. The resulting Green's function has the correct analytical properties (it is real in the band gap between E_v and E_c and complex within the allowed energy bands), and its imaginary part yields the correct free-electron-like densities of states for both conduction and valence bands. This choice of Green's function then determines the embedding potential in the form

$$\Sigma^0 = \Sigma_c^0 + \Sigma_v^0 \tag{29}$$

where Σ_v^0 and Σ_c^0 are the embedding potentials of the free-electron-like valence and conduction bands.

As mentioned in section 3, we take the defect to be a region of semiconductor with a larger band gap ($E_g^{(\mathrm{II})}$) than the rest of the surface (band gap $E_g^{(\mathrm{I})}$). We choose the embedding potential Σ of the surface with defects such that the perturbation potential $\Delta\Sigma(\boldsymbol{x}, \boldsymbol{x}') \neq 0$ if and only if $\boldsymbol{x}$ and $\boldsymbol{x}'$ are located inside the defect region. In that case, we take the embedding potential Σ to be that of another bulk semiconductor with a wider band gap (so that the expressions for the Green's functions are the same as those given above, but with a larger value $E_g^{(\mathrm{II})} > E_g^{(\mathrm{I})}$).

5.1. The one-dimensional embedding potentials $\Sigma^0(k_\parallel)$

For the defect-free surface, we can write a one-dimensional equivalent of equation (2) by exploiting translational symmetry in the surface plane:

$$\Sigma^0(k_\parallel) = g_{(\mathrm{I})}^{-1}(z_0, z_0) - \frac{1}{2}g_{(\mathrm{I})}^{-1}(z_0, z_0)\frac{\mathrm{d}}{\mathrm{d}z'}g_{(\mathrm{I})}(z_0, z')\bigg|_{z'=z_0}. \tag{30}$$

The one-dimensional Green's function $g_{(\mathrm{I})}(z, z')$ is the Fourier transform of the Green's function $G_{(\mathrm{I})}$ of the two-band semiconductor I. Then the embedding potentials Σ_v^0 and Σ_c^0 of the valence and conduction bands are given by

$$\Sigma_v^0 = \begin{cases} +\dfrac{\mathrm{i}}{2}\sqrt{2(E_v - E) - k_\parallel^2} & \text{for } 2(E_v - E) - k_\parallel^2 > 0 \\ -\dfrac{1}{2}\sqrt{2(E - E_v) + k_\parallel^2} & \text{otherwise} \end{cases} \tag{31}$$

and

$$\Sigma_c^0 = \begin{cases} +\dfrac{\mathrm{i}}{2}\sqrt{2(E-E_c)-k_\parallel^2} & \text{for } 2(E-E_c)-k_\parallel^2 > 0 \\ -\dfrac{1}{2}\sqrt{2(E_c-E)+k_\parallel^2} & \text{otherwise.} \end{cases} \tag{32}$$

These forms for the embedding potential are used to calculate the one-dimensional Green's function $g^0(z, z')$ in equation (17).

In principle, the corresponding real-space embedding potential $\Sigma^0(\boldsymbol{x}, \boldsymbol{x}')$ could be obtained by Fourier transforming $\Sigma^0(k_\parallel)$ as in equation (10) or equation (22). However, there is a problem of convergence in the integral of equation (22). Indeed for large $k_\parallel$-values, $\Sigma^0(k_\parallel)$ is proportional to $k_\parallel$ and J_0 to $1/\sqrt{k_\parallel}$. Hence we adopt a different strategy to determine the embedding potential, by using the real-space form which is described next.

5.2. Embedding potentials in real space

As already mentioned in section 2, it is possible to obtain the embedding potential on the separation surface S by considering Green's functions obeying different boundary conditions. Then, instead of working in reciprocal space, we start with a Green's function for the left-hand region (semiconductor I) defined in real space and obeying a Dirichlet boundary condition on the plane $z = z_0$:

$$G_{c,v}(\boldsymbol{r}, \boldsymbol{r}') = -\frac{1}{2\pi}\left(\frac{\mathrm{e}^{\mathrm{i}k_{c,v}|\boldsymbol{r}-\boldsymbol{r}'|}}{|\boldsymbol{r}-\boldsymbol{r}'|} - \frac{\mathrm{e}^{\mathrm{i}k_{c,v}|\boldsymbol{r}-\boldsymbol{r}''|}}{|\boldsymbol{r}-\boldsymbol{r}''|}\right) \tag{33}$$

where the subscripts c, v denote conduction and valence band respectively, and $\boldsymbol{r}''$ is the image of $\boldsymbol{r}'$ in the $z = z_0$ plane. This means that if $\boldsymbol{r}' \equiv (x_1, x_2, z')$ then $\boldsymbol{r}'' \equiv (x_1, x_2, -z')$.

Then the corresponding real-space embedding potential is obtained from the surface derivatives of equation (33) as defined in equation (5). It is easy to show that

$$\Sigma_{c,v}(\boldsymbol{x}, \boldsymbol{x}') = -\frac{1}{4\pi}\left(\frac{\mathrm{e}^{\mathrm{i}k_{c,v}|\boldsymbol{x}-\boldsymbol{x}'|}}{|\boldsymbol{x}-\boldsymbol{x}'|^2}\left[\mathrm{i}k_{c,v} - \frac{1}{|\boldsymbol{x}-\boldsymbol{x}'|}\right]\right). \tag{34}$$

The embedding potential $\Sigma^0(\boldsymbol{x}, \boldsymbol{x}')$ is obtained as the sum of the valence and conduction embedding potentials Σ_v and Σ_c. This means that Σ^0 is a complex (decaying) exponential function of the separation $|\boldsymbol{x} - \boldsymbol{x}'|$ when the energy E lies inside (outside) one of the bands. Finally the perturbation potential $\Delta\Sigma$ used in the Dyson equation, equation (9), is determined from

$$\Delta\Sigma(\boldsymbol{x}, \boldsymbol{x}') = \Sigma(\boldsymbol{x}, \boldsymbol{x}') - \Sigma^0(\boldsymbol{x}, \boldsymbol{x}'). \tag{35}$$

The mathematical forms of Σ and Σ^0 are the same; only the band gaps $E_g^{(\mathrm{II})}$ and $E_g^{(\mathrm{I})}$ are different. Note that $E_g^{(\mathrm{II})}$ in the defect region is larger than $E_g^{(\mathrm{I})}$.

6. Calculations on a discrete mesh

Knowing the expressions in the real space for the perturbation potential $\Delta\Sigma$ and for the Green's function G^0, we are now able to solve the Dyson equation. There are different ways of solving such an integral equation. However, owing to the localization of the perturbation potential in the defect region, we can conveniently recast the Dyson equation in the form

of matrix equations over a finite set of grid points. Hence we can rewrite equation (9) in the following form:

$$G_{rr'} = G^0_{rr'} + \sum_{ij} G^0_{ri} w_i \, \Delta\Sigma_{ij} \, w_j G_{jr'} \tag{36}$$

where the w_i represent the weights for the numerical integration method used to discretize the integrals. For convenience we use indices $i, j, k, \ldots$ for points lying in the surface plane $z = z_0$ and indices r, r' for other points.

Because of the symmetry of the present problem, it is not necessary to solve the matrix equation on a three-dimensional cubic grid. In order to reduce the matrix sizes and save on computing time, it is sufficient to consider two sets of grids defined on two different planar surfaces, the surface plane $z = z_0$ and another plane $z = z_1$ located further away in the vacuum. Hence in order to obtain the Green's function $G_{rr'}$ in the plane $z = z_1$, we can proceed via a three-step calculation.

(i) The first step consists in determining the Green's function only on the surface plane $z = z_0$; for instance

$$G_{ij} = G^0_{ij} + \sum_{kl} G^0_{ik} w_k \, \Delta\Sigma_{kl} \, w_l G_{lj}. \tag{37}$$

Then the matrix G_{ij} is obtained by inverting the matrix $(1 - G^0 \, \Delta\Sigma)_{ij}$ and multiplying by G^0_{ij}.

(ii) The second step is to choose an r-point in the plane $z = z_1$ and to calculate the vector G^0_{ri}. Then the vector G_{ri} is simply obtained by matrix and vector multiplications:

$$G_{ri} = G^0_{ri} + \sum_{jk} G^0_{rj} w_j \, \Delta\Sigma_{jk} \, w_k G_{ki}. \tag{38}$$

(iii) The last step is in principle to choose another r'-point in the plane $z = z_1$, calculate the vector $G^0_{r'i}$ and then $G_{rr'}$. However, since we are interested in the local density of states, we only have to consider the diagonal matrix elements G_{rr}. The calculations are then reduced since all of the necessary elements are already known (except the number G^0_{rr}).

The second and third steps are repeated for all of the r-points in the plane $z = z_1$. Note that the calculations are also considerably reduced in complexity by the fact that the Green's functions and the embedding potentials are symmetric (i.e. $G_{rr'} = G_{r'r}$ and $\Delta\Sigma_{ij} = \Delta\Sigma_{ji}$).

Although with the previous scheme it seems to be easy to obtain the Green's function in the plane $z = z_1$, some difficulties arise form the fact that the real parts of the Green's function G^0 and the perturbation potential $\Delta\Sigma$ have divergent matrix elements when $\boldsymbol{r} = \boldsymbol{r}'$ and $\boldsymbol{x} = \boldsymbol{x}'$ respectively. From equations (24) and (25), we have

$$\lim_{\boldsymbol{r} \to \boldsymbol{r}'} \operatorname{Re} G^0(\boldsymbol{r}, \boldsymbol{r}') = g \frac{1}{|\boldsymbol{r} - \boldsymbol{r}'|} + \text{constant} \tag{39}$$

where $g = -1/2\pi$. Similarly, from the definition of the embedding potentials (section 5.2), it can been shown that for any energy values

$$\lim_{\boldsymbol{x} \to \boldsymbol{x}'} \operatorname{Re} \Delta\Sigma(\boldsymbol{x}, \boldsymbol{x}') = \Delta \frac{1}{|\boldsymbol{x} - \boldsymbol{x}'|} + \text{constant} \tag{40}$$

where $\Delta = (E_g^{(\mathrm{II})} - E_g^{(\mathrm{I})})/(-4\pi)$. This can be checked from power expansion of equation (34) when $R_\parallel = |\boldsymbol{x} - \boldsymbol{x}'|$ tends to zero. It can be seen from the Dyson integral equation that such singularities can be cancelled analytically in the integrals. However, now all quantities are determined on a finite set of grid points (with a fairly coarse grid spacing) and the continuum limit is only achieved for very small grid spacing. Therefore

the matrix representation of the Dyson equation has to be modified to handle carefully these singularities in the diagonal matrix elements of the Green's function and embedding potentials. In order to treat such singular diagonal matrix elements, we follow the same procedure as given in the appendix of reference [8]. The present modified version of this procedure is described in the appendix to this paper. Then the modified equations for our three-step calculations become as follows.

(i) The corrected equation for the surface Green's function G_{ij} is written to the first order in η as follows (η defining the radius of an elementary circular surface around each singularity point, such a surface being related to the regular grid spacing by $\pi\eta^2 = \delta x \times \delta y$):

$$\begin{aligned} G_{ij} = {} & \left[(1 - \hat{G}^0\,\widehat{\Delta\Sigma})^{-1}\tilde{G}^0\right]_{ij} + g\delta_{ij}\frac{1}{|\epsilon|} \\ & + 2\pi g\eta\left(\left[\widehat{\Delta\Sigma}(1 - \hat{G}^0\,\widehat{\Delta\Sigma})^{-1}\tilde{G}^0\right]_{ij} + \left[\widehat{\Delta\Sigma}(1 - \hat{G}^0\,\widehat{\Delta\Sigma})^{-1}\tilde{G}^0\right]_{ji}\right) \\ & + 2\pi g\eta\left[(1 - \hat{G}^0\,\widehat{\Delta\Sigma})^{-1}\hat{G}^0\,\widehat{\Delta\Sigma}\,\widehat{\Delta\Sigma}(1 - \hat{G}^0\,\widehat{\Delta\Sigma})^{-1}\tilde{G}^0\right]_{ij} \\ & + 2\pi\eta\sum_k\left[(1 - \hat{G}^0\,\widehat{\Delta\Sigma})^{-1}\hat{G}^0\right]_{ik}\Delta_k\left[(1 - \hat{G}^0\,\widehat{\Delta\Sigma})^{-1}\tilde{G}^0\right]_{kj}. \end{aligned} \tag{41}$$

$\tilde{G}^0$ and $\widehat{\Delta\Sigma}$ are the Green's function and perturbation potential matrices where we have removed the real-part singularities of the diagonal matrix elements; and $\hat{G}^0_{ij} = \tilde{G}^0_{ij}w_j$, $\widehat{\Delta\Sigma}_{ij} = \widetilde{\Delta\Sigma}_{ij}\,w_j$. Here Δ_k is equal to Δ as defined in equation (40) when the surface vector labelled k is inside the defect region, and otherwise $\Delta_k = 0$. The second and third lines in equation (41) correspond to corrections due to the singularities associated with the Green's function G^0. They are similar to the correction terms introduced in equation (A9) of reference [8]. Here we have supplementary correction terms (the last line in equation (41)) as compared to equation (A9) of reference [8]. These are due to the singularities of the perturbation potential $\Delta\Sigma$ which are not present in the local perturbation potential considered by Lucas *et al* [8]. These results are exact in the perturbation sense, since we have considered all terms of the Born series expansion of the Dyson equation. However, such correction terms are only expanded to the first order η in the linear spacing of the grid.

(ii) The Dyson equation for the second step of calculation can be written as

$$G_{ri} = \tilde{G}^0_{ri} + \sum_{jk}\tilde{G}^0_{rj}w_j\,\Delta\Sigma_{jk}\,w_kG_{ki}. \tag{42}$$

We can use $\tilde{G}^0$ because any r-vectors lying in the plane $z = z_1$ are different from any i-vectors lying in the plane $z = z_0$. We have to take into account the corrections due to the singularities of $\Delta\Sigma_{jk}$ and G_{ki} which give us

$$\tilde{G}_{ri} = \tilde{G}^0_{ri} + \sum_{jl}\hat{G}^0_{rj}\,\widehat{\Delta\Sigma}_{jl}\,\tilde{G}_{li} + 2\pi\eta\sum_j\hat{G}^0_{rj}\Delta_j\tilde{G}_{ji} + 2\pi g\eta\sum_j\widehat{\Delta\Sigma}_{ij}\,\tilde{G}^0_{jr}. \tag{43}$$

$\tilde{G}_{ij}$ is obtained from equation (41) by suppressing the diagonal singularity $\delta_{ij}/|\epsilon|$.

(iii) Finally the third step of the calculation is

$$G_{rr} = \tilde{G}^0_{rr} + g\delta_{rr}\frac{1}{|\epsilon|} + \sum_{jk}\tilde{G}^0_{rj}w_j\,\Delta\Sigma_{jk}\,w_k\tilde{G}_{kr} \tag{44}$$

which in its corrected form gives

$$G_{rr} = \tilde{G}^0_{rr} + g\delta_{rr}\frac{1}{|\epsilon|} + \sum_{jl}\hat{G}^0_{rj}\,\widehat{\Delta\Sigma}_{jl}\,\tilde{G}_{lr} + 2\pi\eta\sum_j\hat{G}^0_{rj}\Delta_j\tilde{G}_{jr}. \tag{45}$$

Equations (41), (43) and (45) are now used to determine the local density of states $n(E, r) = -(1/\pi)\,\mathrm{Im}\,G_{rr}(E)$ from the imaginary part of the Green's function G_{rr} on the plane $z = z_1$.

7. The adsorbate with an axial symmetry

In this section, we consider a particular symmetry for the defect region. This region is chosen to be a circle of radius R centred at the origin. According to the axial symmetry of the system, every important quantity such as the wave functions, the Green's functions and the embedding potentials can be represented by harmonic expansions, owing to the invariance of such quantities under variation of the value of the angle ϕ between any two two-dimensional vectors $\boldsymbol{x} = (\rho, \phi)$. The physics and the procedures that we have derived in the previous sections are not modified in principle. In this section, we just give the harmonic representation of the relevant equations.

Hence the Green's functions and the embedding (or perturbing) potentials, represented by the function $f(\boldsymbol{x}, \boldsymbol{x}')$, are expanded as follows:

$$f(\boldsymbol{x}, \boldsymbol{x}') = \sum_{m=-\infty}^{+\infty} f_m(\rho, \rho', z, z')\mathrm{e}^{\mathrm{i}m(\phi-\phi')}. \tag{46}$$

According to the Graf addition theorem [17]:

$$J_0(k_\parallel|\boldsymbol{x} - \boldsymbol{x}'|) = \sum_m J_m(k_\parallel\rho)J_m(k_\parallel\rho')\mathrm{e}^{\mathrm{i}m(\phi-\phi')} \tag{47}$$

the harmonic decomposition of equation (24) is

$$g_m^0(\rho, \rho', z, z') = g_m^f(\rho, \rho', z, z') + \frac{1}{2\pi}\int_0^{k_\parallel^{\max}} \mathrm{d}k_\parallel\ k_\parallel J_m(k_\parallel\rho)J_m(k_\parallel\rho')\left[g^0(z, z') - g^f(z, z')\right]. \tag{48}$$

Finally using the orthogonality relation

$$\int_{-\pi}^{+\pi} \mathrm{d}\phi_1\ \mathrm{e}^{\mathrm{i}(m-m')\phi_1} = 2\pi\delta_{m,m'} \tag{49}$$

we obtain the following Dyson equation for each mth-harmonic component (harmonic decomposition of equation (9)):

$$g_m(\rho, \rho', z, z') = g_m^0(\rho, \rho', z, z') + (2\pi)^2\int_0^R \mathrm{d}\rho_1\ \rho_1\int_0^R \mathrm{d}\rho_2\ \rho_2 g_m^0(\rho, \rho_1, z, z_0) \times\ \Delta\sigma_m(\rho_1, \rho_2)g_m(\rho_2, \rho', z_0, z') \tag{50}$$

where $\Delta\sigma_m$ is the mth-harmonic component of $\Delta\Sigma$ obtained from equation (46).

Then we have to determine an equivalent procedure to treat the singularities of the Green's function g_m^0 and the perturbation potential $\Delta\sigma_m$. The singularities in g_m^0 arise from g_m^f, and the latter is calculated from the inverse of equation (46) via

$$g_m^f(\rho, \rho', z, z') = \frac{g}{\pi}\int_0^\pi \mathrm{d}\phi_1\ \cos(m\phi_1)\frac{\mathrm{e}^{\mathrm{i}K(a-b\cos\phi_1)^{1/2}}}{(a - b\cos\phi_1)^{1/2}} \tag{51}$$

where $a = \rho^2 + \rho'^2 + (z - z')^2$ and $b = 2\rho\rho'$. Such an integral is well behaved except when $a = b$. It can be seen that in such a case, the imaginary part of the integrand has a finite value for $\phi_1 = 0$, and consequently it can be integrated without any difficulties. However, the real part diverges as $(a - b\cos\phi_1)^{-1/2}$. In equation (51) the real-part singularity arises at

around $\phi_1 = 0$ (when $a = b$), and hence the integral can be approximated by the following one:

$$\frac{g}{\pi}\int_0^{\pi} \mathrm{d}\phi_1 \; \frac{1}{\sqrt{a - b\cos\phi_1}}. \tag{52}$$

This integral is a complete elliptic integral of the first kind, and according to equations (61)–(63) of reference [8], one obtains a logarithmic singularity for the Green's function. Then considering a power expansion of the perturbation potential $\Delta\Sigma(\boldsymbol{x}, \boldsymbol{x}')$ when $\boldsymbol{x} \to \boldsymbol{x}'$, it can be seen that the corresponding imaginary part also has a finite value when $a = b$ and $\phi_1 = 0$, and that the real part diverges in the same way as the Green's function g_m^f. Hence we obtain for the real part of both the perturbation potential $\Delta\sigma_m$ and the Green's function g_m^0 the following logarithmic singularity:

$$\lim_{\epsilon\to 0} \mathrm{Re}\begin{bmatrix} g_m^0 \\ \Delta\sigma_m \end{bmatrix}(\boldsymbol{x}, \boldsymbol{x}+\epsilon) = -\frac{1}{\pi\rho}\ln\left(\frac{\epsilon}{8\rho}\right)\begin{bmatrix} g \\ \Delta \end{bmatrix}. \tag{53}$$

The harmonic expansion equation (50) of the Dyson equation can then be corrected using a procedure similar to that given in the appendix. Here the one-dimensional integrals $\int \mathrm{d}\rho$ are decomposed into different segments. We define small segments (of length η) around points where the singularities occur. The latter can be evaluated analytically from the following elementary integral:

$$\int_0^{\eta} \mathrm{d}\epsilon \; \epsilon \ln\left(\frac{\epsilon}{8\rho}\right) = \frac{1}{4}\eta^2\left(\ln\left(\frac{\eta}{8\rho}\right)^2 - 1\right). \tag{54}$$

This equation is the analogue of equation (A3). Then we obtain for the m-component of the harmonic expansion of the Dyson equation defined on the surface plane S

$$\begin{aligned}\tilde{g}_{m,ij} = {} & \left[(1 - \hat{g}_m^0\,\widehat{\Delta\sigma}_m)^{-1}\tilde{g}_m^0\right]_{ij} + 2\pi g\left(c(\rho_i)\left[\widehat{\Delta\sigma}_m(1 - \hat{g}_m^0\,\widehat{\Delta\sigma}_m)^{-1}\tilde{g}_m^0\right]_{ij}\right) \\ & + 2\pi g\left(c(\rho_j)\left[\widehat{\Delta\sigma}_m(1 - \hat{g}_m^0\,\widehat{\Delta\sigma}_m)^{-1}\tilde{g}_m^0\right]_{ji}\right) \\ & + 2\pi g\left[(1 - \hat{g}_m^0\,\widehat{\Delta\sigma}_m)^{-1}\hat{g}_m^0\,\widehat{\Delta\Sigma}\,c(\rho)\,\widehat{\Delta\Sigma}(1 - \hat{g}_m^0\,\widehat{\Delta\sigma}_m)^{-1}\tilde{g}_m^0\right]_{ij} \\ & + 2\pi\sum_k \left[(1 - \hat{g}_m^0\,\widehat{\Delta\sigma}_m)^{-1}\hat{g}_m^0\right]_{ik}\Delta_k c(\rho_k)\left[(1 - \hat{g}_m^0\,\widehat{\Delta\sigma}_m)^{-1}\tilde{g}_m^0\right]_{kj}\end{aligned} \tag{55}$$

where

$$c(\rho) = \frac{1}{4\pi\rho}\eta^2\left(1 - \ln\left(\frac{\eta}{8\rho}\right)^2\right). \tag{56}$$

Again $\Delta_k = \Delta$ if and only if $0 \leqslant \rho_k \leqslant R$ and otherwise $\Delta_k = 0$. We have used the factorizations

$$\hat{g}_{m,ij}^0 = \tilde{g}_{m,ij}^0\, 2\pi\, w_j \rho_j \tag{57}$$

and

$$\widehat{\Delta\sigma}_{m,ij} = \widetilde{\Delta\sigma}_{m,ij}\, 2\pi\, w_j \rho_j \tag{58}$$

where $\tilde{g}_m^0$ and $\widetilde{\Delta\sigma}_m$ are the m-components of the harmonic expansions of G^0 and $\Delta\Sigma$ respectively, where we have suppressed the logarithmic singularity of the diagonal elements. The equivalent harmonic expansions of equations (43) and (45) are straightforward to obtain when one considers equation (55).

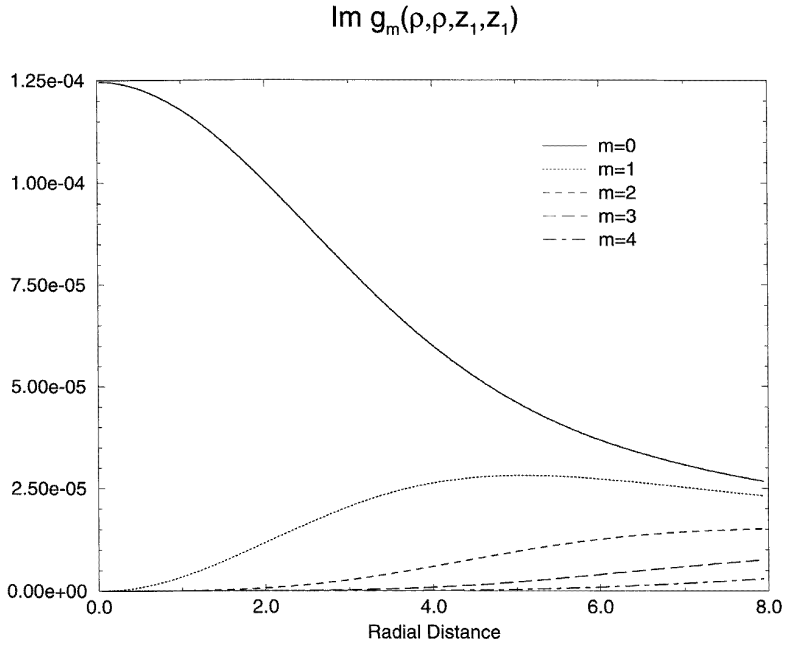

Figure 2. The negative of the imaginary part of the harmonic component $g_m(\rho, \rho, z_1, z_1)$ versus the radial distance ρ in Å. The value of the electric field is $\xi^{\text{ext}} = -0.9$ V Å^{-1}. The energy is close to the top of the valence band of semiconductor I. The location of the plane $z = z_1$ ($z_1 = 2.65$ Å) is inside the tunnelling barrier. $m = 0$: full line; $m = 1$: dotted line; $m = 2$: dashed line; $m = 3$: long-dashed line; and $m = 4$: chain line.

8. Results

As a first study, we consider a circular defect deposited on the surface of semiconductor I. Therefore we use the formalism described in section 7 to determine the local density of states in a plane located in the vacuum. The values for the different parameters that we use have been chosen from the literature to be typical of hydrocarbon molecules deposited on silicon. For example, semiconductor I is represented by a silicon crystal with a band gap of $E_g^{(\text{I})} = 1.12$ eV and a work function of $W = 4.5$ eV. The defect region is considered to be a semiconductor with a gap larger than $E_g^{(\text{I})}$. Most of the organic (alkane-like) crystals have band gaps ranging from 4 to 10 eV. Therefore we take for $E_g^{(\text{II})}$ an intermediate value: $E_g^{(\text{II})} = 6.0$ eV, the latter being in agreement with the energy difference between the HOMO and LUMO states obtained for a single isolated ethylene molecule in LDA calculations. The radius of the defect region is chosen to be $R = 2.3$ Å which is approximately the radius of a circular region covering an adsorbed ethylene molecule on the silicon surface. Finally, the values of the external applied electric field are deduced from typical STM experimental conditions. It is reasonably assumed that typical bias values range between 1 and 3 V, and estimated tip–sample distances between 2 and 6 Å. Hence the corresponding tip-induced electric field ξ^{ext} varies approximately between 0.16 and 1.50 eV Å^{-1}. In order to simulate STM experiments in which the electrons tunnel out of the surface, negative values for ξ^{ext} have been taken and the corresponding Green's functions are calculated for energies

E close to the top of the valence band of semiconductor I, but within the band gap of semiconductor II.

Figure 2 represents the (negative of the) imaginary part of several harmonic components $g_m(\rho, \rho, z_1, z_1)$ in the plane $z_1 = 2.65$ Å. Note that in this case, the value of z_1 is lower than the value of the classical turning point $z_{\text{tp}} = (W - E)/|\xi^{\text{ext}}|$, i.e. the plane $z = z_1$ is located inside the tunnelling barrier. The general shape of the different g_m is reminiscent of that of the integral of $J_m^2(x)$ as found in equation (48). The Green's function G_{rr} is calculated from equation (46). However, due to the symmetry of the Green's function, G_{rr} can be obtained from

$$G_{rr} = g_0(\rho, \rho, z_1, z_1) + 2\sum_{m=1}^{+\infty} g_m(\rho, \rho, z_1, z_1). \tag{59}$$

It is not necessary to perform the summation in equation (59) to infinity; G_{rr} can be obtained with a very good accuracy by considering only the first few harmonic components. In practice, the summation runs from $m = 0$ to $m_{\max} = 10$.

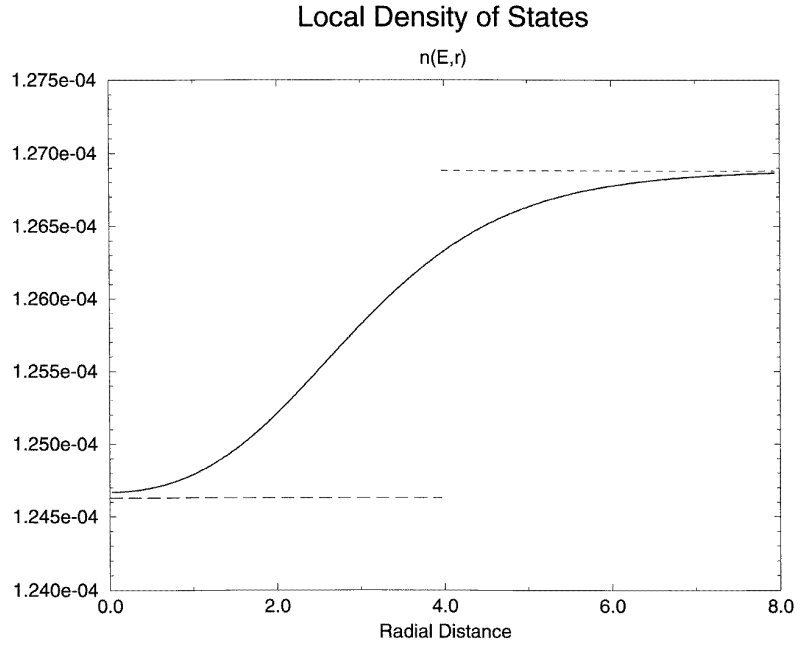

Figure 3. The local density of states $n(E, r)$ calculated from the g_m-components shown in figure 2 versus the radial distance ρ given in Å. The corresponding values of $n(E, r)$ for the perfect surface with the gaps $E_g^{(\text{I})}$ and $E_g^{(\text{II})}$ are represented respectively by the short-dashed and long-dashed lines.

The corresponding local density of states $n(E, r)$ is shown in figure 3. As expected, the value of $n(E, r)$ for a surface that does not contain defects (the semiconductor surface with the gap $E_g^{(\text{I})}$) is recovered far from the defect ($\rho \gg R$). At the centre of the defect ($\rho = 0$), the value of $n(E, r)$ is almost equal to that of the semiconductor surface with the gap $E_g^{(\text{II})}$ (strictly equal in the case of large values of the defect radius R). Note that the modification of the local density of states due the defect extends over a larger distance than the defect

radius itself. The fact that the density-of-states values above the region with defects are smaller is essentially due to the fact that the defect has a band gap larger than that of the surface itself.

The same trends have been observed for different values of the energy E and for different locations of the plane $z = z_1$ (inside and outside of the tunnelling barrier). Of course, the larger the energy difference $W - E$ is (and the further the plane $z = z_1$ is placed away from the surface plane), the lower the values of $n(E, r)$ become.

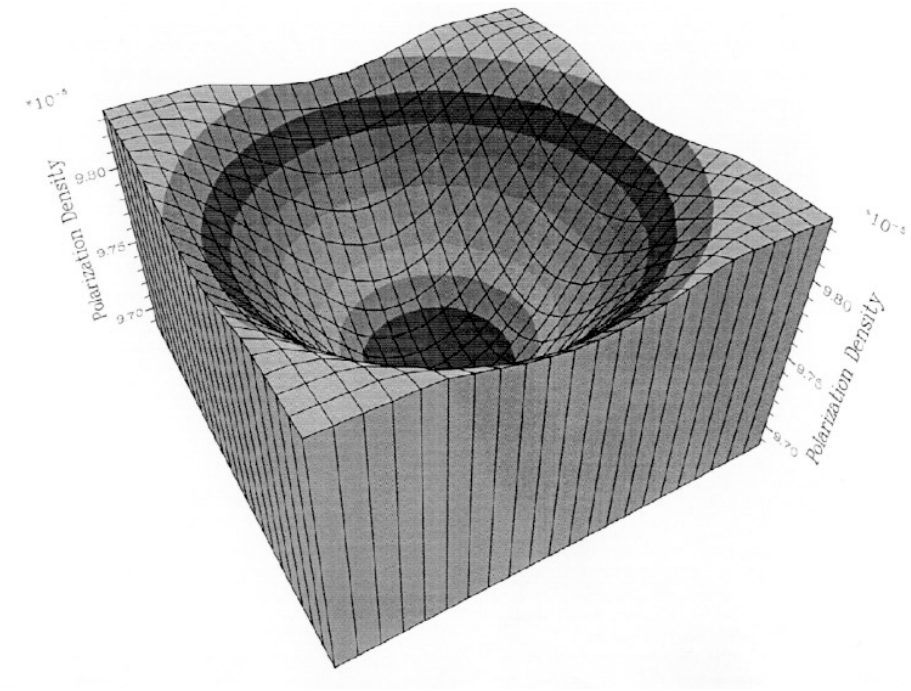

Figure 4. A 3D view of the polarization local density of states Δn in the plane $z = z_1$. Δn is calculated from the two different values of the electric field $\xi_1^{\text{ext}} = -0.90$ V Å^{-1} and $\xi_2^{\text{ext}} = -0.77$ V Å^{-1}.

By increasing the (absolute) value of the electric field ξ^{ext}, one reduces the tunnelling barrier width, and consequently the values of the local density of states increase in the vacuum. In order to quantify the influence of ξ^{ext} on the local density of states above the bare surface and the defect, we consider the polarization density of states Δn defined by

$$\Delta n(E, r) = n(E, r)|_{\xi_1^{\text{ext}}} - n(E, r)|_{\xi_2^{\text{ext}}} \qquad \text{where } \xi_1^{\text{ext}} > \xi_2^{\text{ext}}. \tag{60}$$

(It is convenient to compare the results for two non-zero values of ξ^{ext} because the formulation in terms of Airy functions becomes singular at $\xi^{\text{ext}} = 0$.) A typical example of the behaviour of the polarization density of states is shown in figure 4. These results definitively show that the influence of the electric field is more important above the bare surface than above the defect, since we observe a relative suppression of the local density of states above the defect region. In other words, due to the electric field, the 'spreading' of electronic states in the vacuum is less important above the defect region than above the bare surface. Such a behaviour has been already obtained in our previous study of adsorbed

ethylene molecules on the Si(001) surface using *ab initio* calculations [4]. This behaviour reminds us of the fact that the defect has a band gap larger than that of the bare surface itself, i.e. the defect is less polarizable than the bare surface.

9. Conclusion

In this paper, we have studied the influence of an external electric field on the electronic structure of a surface with defects made up of semiconductors. A general approach to determining the Green's function for such a complex system has been presented. The method combines the use of embedding potentials and the resolution of the Dyson equation on a discrete mesh. As a first step, we have used simple (but not the simplest) forms for the embedding potentials of the surface and defect regions. These have been represented by two-band semiconductors. The polarization of the surface with defects has been studied in the 'non-classical' regime. It has been found that the response of the electronic states to the tip-induced electric field is spatially modulated by the surface and the defect (adsorbate), the defect being less polarizable than the bare surface itself. This behaviour is in agreement with *ab initio* calculations performed for ethylene molecules adsorbed on a Si(001) surface [4]. Improvements of the present embedding approach are still possible. An atomic description of an adsorbate deposited on a jellium surface has been proposed in the recent work of Trioni *et al* [18]. However, for an atomic description of both the adsorbate and the surface, an *ab initio* slab calculation is straightforward [4].

Acknowledgments

We thank Dr G A D Briggs for a number of discussions of his experimental results. We are grateful to the Engineering and Physical Science Research Council for support under grants GR/J67734 and GR/K80495.

Appendix

In this appendix, we show how to treat the singularities of the diagonal elements of the Green's function G^0 and the perturbation potential $\Delta\Sigma$ defined respectively by equations (39) and (40). First we consider the Born series expansion of the Dyson equation, equation (9). For the vectors $\boldsymbol{x}$ and $\boldsymbol{x}'$ lying in the surface plane $z = z_0$ (also denoted as S), the first term of the Born series $G^{(1)}(\boldsymbol{x}, \boldsymbol{x}')$ is written as

$$G^{(1)}(\boldsymbol{x}, \boldsymbol{x}') = \int_S \mathrm{d}^2\boldsymbol{x}_1 \int_S \mathrm{d}^2\boldsymbol{x}_2 \; G^0(\boldsymbol{x}, \boldsymbol{x}_1)\, \Delta\Sigma(\boldsymbol{x}_1, \boldsymbol{x}_2)\, G^0(\boldsymbol{x}_2, \boldsymbol{x}'). \tag{A1}$$

The integrals $\int_S \mathrm{d}^2\boldsymbol{x}_1$ and $\int_S \mathrm{d}^2\boldsymbol{x}_2$ are decomposed into different parts wherein the singularities can be treated analytically. Each singularity of G^0 or $\Delta\Sigma$ is treated separately. Starting with $\int_S \mathrm{d}^2\boldsymbol{x}_2$ we have

$$\begin{aligned}\int_S \mathrm{d}^2\boldsymbol{x}_2 \; \Delta\Sigma(\boldsymbol{x}_1, \boldsymbol{x}_2)\, G^0(\boldsymbol{x}_2, \boldsymbol{x}') &= \int_{S'} \mathrm{d}^2\boldsymbol{x}_2 \; \Delta\Sigma(\boldsymbol{x}_1, \boldsymbol{x}_2)\, G^0(\boldsymbol{x}_2, \boldsymbol{x}') \\ &+ \Delta\Sigma(\boldsymbol{x}_1, \boldsymbol{x}') \int_{S\boldsymbol{x}'} \mathrm{d}^2\boldsymbol{x}_2 \; \frac{g}{|\boldsymbol{x}_2 - \boldsymbol{x}'|} + G^0(\boldsymbol{x}_1, \boldsymbol{x}') \int_{S\boldsymbol{x}_1} \mathrm{d}^2\boldsymbol{x}_2 \; \frac{\Delta}{|\boldsymbol{x}_1 - \boldsymbol{x}_2|}\end{aligned} \tag{A2}$$

where $S\boldsymbol{x}_1$ ($S\boldsymbol{x}'$) represents a small circular region of radius η centred around $\boldsymbol{x}_1$ ($\boldsymbol{x}'$) respectively. $\int_{S'}$ is a surface integral over the surface plane S excluding these two small circular regions ($S' = S - S\boldsymbol{x}_1 - S\boldsymbol{x}'$).

In the limit of small η-values, the integrals in the second line of equation (A2) can be evaluated analytically. For example,

$$\int_{S\boldsymbol{x}'} \mathrm{d}^2\boldsymbol{x}_2 \; g\frac{1}{|\boldsymbol{x}_2 - \boldsymbol{x}'|} = g\int_0^{2\pi}\mathrm{d}\phi\int_0^{\eta}\mathrm{d}\epsilon\;\epsilon\frac{1}{\epsilon} = 2\pi g\eta \tag{A3}$$

where we write symbolically $\boldsymbol{x}_2 = \boldsymbol{x}' + \epsilon$. The radius η of the circular regions is related to the regular grid spacing δx and δy by $\pi\eta^2 = \delta x \times \delta y$.

Then we can treat the $\int_S \mathrm{d}^2\boldsymbol{x}_1$ integral in equation (A1) in the same manner as previously. Keeping only the terms in the first order of η, we obtain for equation (A1) the following corrected version:

$$\begin{aligned} G^{(1)}(\boldsymbol{x},\boldsymbol{x}') = {} & \int_S \mathrm{d}^2\boldsymbol{x}_1\int_S \mathrm{d}^2\boldsymbol{x}_2\;\tilde{G}^0(\boldsymbol{x},\boldsymbol{x}_1)\,\widetilde{\Delta\Sigma}(\boldsymbol{x}_1,\boldsymbol{x}_2)\,\tilde{G}^0(\boldsymbol{x}_2,\boldsymbol{x}') \\ & + 2\pi g\eta\int_S \mathrm{d}^2\boldsymbol{x}_1\;\tilde{G}^0(\boldsymbol{x},\boldsymbol{x}_1)\,\widetilde{\Delta\Sigma}(\boldsymbol{x}_1,\boldsymbol{x}') + \widetilde{\Delta\Sigma}(\boldsymbol{x},\boldsymbol{x}_1)\,\tilde{G}^0(\boldsymbol{x}_1,\boldsymbol{x}') \\ & + 2\pi\eta\int_S \mathrm{d}^2\boldsymbol{x}_1\;\tilde{G}^0(\boldsymbol{x},\boldsymbol{x}_1)\Delta(\boldsymbol{x}_1)\tilde{G}^0(\boldsymbol{x}_1,\boldsymbol{x}') \end{aligned} \tag{A4}$$

where $\tilde{G}^0$ and $\widetilde{\Delta\Sigma}$ are the corresponding Green's function and perturbation potential, where we have removed the singularities of the diagonal elements. $\Delta(\boldsymbol{x}_1)$ is equal to Δ defined in equation (40) if and only if $\boldsymbol{x}_1$ is located in the defect region; otherwise $\Delta(\boldsymbol{x}_1) = 0$. Then treating all orders of perturbation in the Born series expansion, and keeping terms up to order η, we obtain the corrected Dyson equation on the surface plane S. As an illustration we give the corrected expression for the second term of the Born series:

$$\begin{aligned} G^{(2)}(\boldsymbol{x},\boldsymbol{x}') &= \left[G^0\,\Delta\Sigma\,G^0\,\Delta\Sigma\,G^0\right]_{\boldsymbol{x},\boldsymbol{x}'} \\ &= \left[\tilde{G}^0\,\widetilde{\Delta\Sigma}\,\tilde{G}^0\,\widetilde{\Delta\Sigma}\,\tilde{G}^0\right]_{\boldsymbol{x},\boldsymbol{x}'} + 2\pi\eta\left[\tilde{G}^0\,\Delta\,\tilde{G}^0\,\widetilde{\Delta\Sigma}\,\tilde{G}^0 + \tilde{G}^0\,\widetilde{\Delta\Sigma}\,\tilde{G}^0\,\Delta\,\tilde{G}^0\right]_{\boldsymbol{x},\boldsymbol{x}'} \\ &\quad + 2\pi g\eta\left[\widetilde{\Delta\Sigma}\,\tilde{G}^0\,\widetilde{\Delta\Sigma}\,\tilde{G}^0 + \tilde{G}^0\,\widetilde{\Delta\Sigma}\,\tilde{G}^0\,\widetilde{\Delta\Sigma}\right]_{\boldsymbol{x},\boldsymbol{x}'} \\ &\quad + 2\pi g\eta\left[\tilde{G}^0\,\widetilde{\Delta\Sigma}\,\widetilde{\Delta\Sigma}\,\tilde{G}^0\right]_{\boldsymbol{x},\boldsymbol{x}'}. \end{aligned} \tag{A5}$$

The corrections propagate throughout the entire Born series expansion. Such correction terms can therefore be resummed or factorized. According to the appendix of reference [8], we obtain the closed form for the corrected Dyson equation in the surface plane S, which is given in the matrix representation by equation (41).

References

[1] Binnig G, Rohrer H, Gerber C and Weibel E 1982 *Phys. Rev. Lett.* **49** 57

[2] Tersoff J and Hamann D R 1985 *Phys. Rev.* B **31** 805
Tsukada M and Shima N 1987 *J. Phys. Soc. Japan* **56** 2875

[3] See, for example:
Doyen G, Drakova D and Scheffler M 1993 *Phys. Rev.* B **47** 9778
Joachim C, Sautet P and Lagier P 1992 *Europhys. Lett.* **20** 697
Noguera C 1991 *Phys. Rev.* B **43** 11 612
Todorov T N, Briggs G A D and Sutton A P 1993 *J. Phys.: Condens. Matter* **5** 2389

[4] Ness H and Fisher A J 1997 *Surf. Sci. Lett.* at press

[5] Mayne A J, Avery A R, Knall J, Jones T S, Briggs G A D and Weinberg W H 1993 *Surf. Sci.* **284** 247

[6] Mayne A J 1994 *DPhil* University of Oxford
[7] Inglesfield J E 1981 *J. Phys. C: Solid State Phys.* **14** 3795
[8] Lucas A A, Morawitz H, Henry G R, Vigneron J P, Lambin P, Cutler P H and Feuchtwang T E 1988 *Phys. Rev.* B **37** 10 708
[9] Garcia-Moliner F and Rubio J 1969 *J. Phys. C: Solid State Phys.* **2** 1789
[10] Inglesfield J E 1971 *J. Phys. C: Solid State Phys.* **4** L14
Inglesfield J E 1972 *J. Phys. F: Met. Phys.* **2** 878
[11] Heine V 1980 *Solid State Physics* vol 35 (New York: Academic) p 19
[12] Noguera C 1990 *Phys. Rev.* B **42** 1629
[13] Tekman E 1992 *Phys. Rev.* B **46** 4938
[14] Fisher A J 1990 *J. Phys.: Condens. Matter* **2** 6079
[15] Abramowitz M and Stegun I A (ed) 1972 *Handbook of Mathematical Functions* (New York: Dover) p 446
[16] Arfken G 1985 *Mathematical Methods For Physicists* 3rd edn (New York: Academic) p 897
[17] Abramowitz M and Stegun I A (ed) 1972 *Handbook of Mathematical Functions* (New York: Dover) p 363
[18] Trioni M I, Brivio G P, Crampin S and Inglesfield J E 1996 *Phys. Rev* B **53** 8052